

# THEORETICAL DESCRIPTION OF HIGH-LYING TWO-ELECTRON STATES

Chris H. Greene

*Department of Physics and Joint Institute for Laboratory Astrophysics  
University of Colorado, Boulder, Colorado 80309-0440*

Michael Cavagnero

*Department of Physics and Astronomy  
University of Kentucky, Lexington, Kentucky 40506-0055*

H. R. Sadeghpour

*Harvard-Smithsonian Center for Astrophysics  
60 Garden Street, Cambridge, Massachusetts 02138*

## ABSTRACT

Within the past two years, experiments on high-lying doubly-excited states in He and  $H^-$  have shown spectra at energies near excited hydrogenic thresholds having principal quantum numbers in the range  $N = 5 - 9$ . While they display some nontrivial complexities, the spectra are tremendously simpler than might be anticipated on the basis of independent electron models, in that only a small fraction of the total number of anticipated resonances are observed experimentally. Moreover, for principal quantum numbers  $N$  that are not too high, specifically  $N < 5$  in He and  $N < 10$  in  $H^-$ , the resonance positions are described accurately by adiabatic calculations using hyperspherical coordinates and can be parametrized by a remarkably simple two-electron Rydberg formula. The observed propensity for excitation of only a small subset of the possible resonance states has been codified by several groups into approximate selection rules based on alternative (but apparently equivalent) classification schemes. Comparatively few attempts have been made at quantitative tests of the validity of these rules. The present review describes recent efforts to quantify their accuracy and limitations using R-matrix and quantum defect techniques, and Smith's delay-time matrix. Propensity rules for exciting different degrees of freedom are found to differ greatly in their degree of validity.

## INTRODUCTION

In just the last few years our understanding of the most fundamental and most common Coulombic three-body systems He and  $H^-$  has taken rapid strides forward, driven particularly by rapid experimental progress.<sup>1,2</sup> In the case of  $H^-$ , the LAMPF experiment of Harris *et al.*<sup>2</sup> showed that in one-photon absorption by the ground state (which reaches final states of  $^1P^o$  symmetry), resonance states are observed only within the lowest  $+$  channel approaching each hydrogenic threshold. These are the  $+$  states in the lowest quantum of bending vibration of the two electrons. This interpretation emerged by comparing the experimental resonance positions with theoretical positions calculated in the adiabatic hyperspherical potential curves<sup>3,4</sup> shown in Fig. 1(a). A great deal of complexity is apparent in these calculated potential curves. For  $^1P^o$  symmetry, there are  $2N - 1$  potential

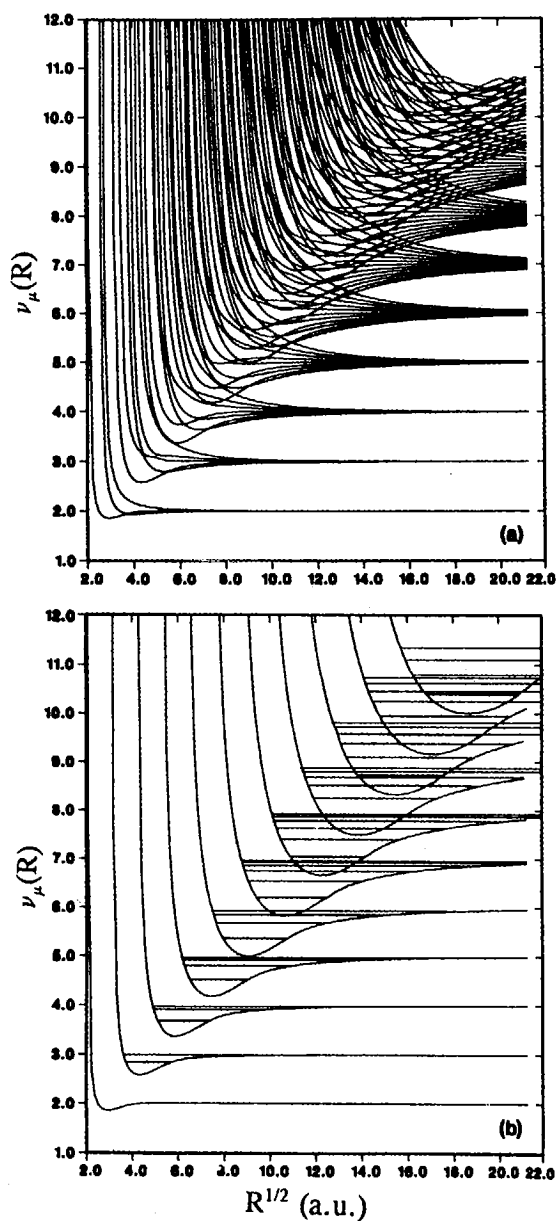


Fig. 1. Adiabatic hyperspherical potential curves for  $1P^o$  symmetry of  $H^-$ , shown as an effective quantum number versus the square root of the hyper-radius  $R$  in atomic units. The complete set of potential curves converging to all  $N > 1$  is shown in (a), while in (b) only the propensity-favored excitation channels are indicated along with the resonance energies calculated in an adiabatic hyperspherical approximation. From Ref. 3.

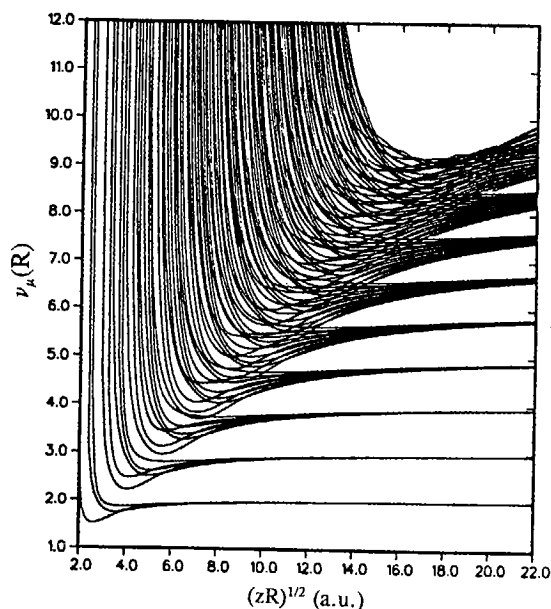


Fig. 2. Same as Fig. 1(a), except for doubly-excited  $1P^o$  channels of He. The hyperradius  $R$  has been rescaled by the nuclear charge  $z = 2$ .

curves converging at  $R \rightarrow \infty$  to each degenerate hydrogenic threshold  $N$ . Of these numerous curves, the one that connects asymptotically to the second-most attractive potential curve is the first  $+$  state in the  $N$ -manifold, owing to a ubiquitous  $+/-$  crossing for  $1P^o$  symmetry identified first by Macek.<sup>5</sup> Only states supported by these potential curves are seen experimentally, whereby the full complexity of Fig. 1(a) can be replaced for practical purposes by the tremendously simpler Fig. 1(b). A somewhat surprising result is the fact that for  $N$ -manifolds having more than one  $+$  state, only the lowest is excited, i.e. the one that is nodeless in the bending vibrational quantum number  $v$  of the electron pair. Higher  $+$  states in an excited bending state are simply not observed, a difficult fact to interpret from the potential curves alone since all of the  $+$  potential curves look very similar. The molecular model of Rost, Feagin, and Briggs<sup>6</sup> interprets this propensity as a conservation of the number of angular nodal lines in spheroidal coordinates, which amounts to the same qualitative interpretation given in Refs. 3 and 4 in terms of the bending vibrational quanta.

These basic conclusions were verified and extended by the measurements of Domke *et al.*,<sup>1</sup> using synchrotron radiation to photoionize the helium ground state in the energy range near the higher thresholds of  $\text{He}^+(N)$ , with  $N = 2 - 6$ . The relevant helium  $1P^o$  potential curves calculated by Sadeghpour<sup>4</sup> are shown in Fig. 2. They demonstrate the same qualitative trend seen in  $\text{H}^-$ , in that the lowest  $+$  potential curve within each  $N$ -manifold is the dominant one observed in the resonance spectrum. Unlike  $\text{H}^-$ , a small number of states with excited bending

ity of  $\text{H}^-$ , shown  
hyper-radius  $R$   
g to all  $N > 1$  is  
channels are indi-  
c hyperspherical

quanta ( $v = 1$ ) were observed in helium, possibly indicating that the propensity rule for exciting only  $v = 0$  states is weaker in He than in  $H^-$ , or else reflecting the higher spatial overlap between the ground state and the lowest  $v = 1$  channels in He.

One new result of the combined theoretical and experimental study of Ref. 1 was the realization that the spectrum showed a new type of interference between resonances belonging to different  $N$ -manifolds. This sort of interference or "perturbation" is very familiar in multichannel Rydberg spectra of the alkaline earth atoms,<sup>7</sup> and it is seen very clearly in the data of Domke *et al.*<sup>1</sup> shown in Fig. 3. The spectrum in Fig. 3(c) covers the energy range between the  $N = 4$  and  $N = 5$  thresholds, where the lowest state in the  $N = 6$  manifold (often called the "Wannier ridge state") is embedded in the middle of the Rydberg series members converging to the  $N = 5$  ionization threshold. Figure 3(a,b) shows the more typical unperturbed spectrum below the  $N = 3, 4$  thresholds consisting of regularly spaced Rydberg lines having comparable peak intensity but whose widths decrease as  $\nu^{-3}$ , where  $\nu$  is the effective quantum number of the outermost Rydberg electron. (When the width becomes smaller than the experimental energy resolution, the peak heights are seen to gradually fall off.)

The perturbation of the  $N = 5$  Rydberg series members by the Wannier ridge state of the  $N = 6$  manifold was anticipated in Ref. 3 by making use of the fact that the observed two-electron resonance states fit a remarkably regular two-electron Rydberg formula with only two adjustable parameters. The formula takes a very different form for He and  $H^-$ . For He, it is derived by starting from the formula of Read<sup>8</sup> and of Rau<sup>9</sup> for the Wannier ridge states alone (i.e., those having comparable radial excitations of both electrons). This formula was introduced phenomenologically in Refs. 8,9 with two empirical constants to be fitted to experimental energies. (A deeper understanding of the origin of this energy level formula was subsequently derived by Lin and Watanabe.<sup>10</sup> The most satisfactory explanation came out of a semiclassical first-principles derivation by Wintgen *et al.*,<sup>11</sup> in which no undetermined empirical constants remain to be fitted to experiment.) The ridge state of principal quantum number  $N$  is now assumed to be the lowest member of a *one-electron* Rydberg series converging to the threshold  $He^+(N)$  with a constant quantum defect. This gives a Rydberg formula which describes all of the propensity-favored two-electron resonance states. [For  $^1P^o$ , these are the ones having  $T = 1$ ,  $K = N - 2$ , and  $A = +$ , in the  $(K, T)^A$  classification scheme of Herrick<sup>12</sup> as extended and reinterpreted by Lin.<sup>13</sup> We advocate<sup>3,4</sup> replacing the  $K$  quantum number by the number of bending vibrational nodes  $v = \frac{1}{2}(N - K - T - 1)$  because the corresponding propensity rule can then be stated as  $\Delta v = 0$  for nonadiabatic transitions between potential curves of the type shown in Figs. 1 and 2.] The resulting two-electron Rydberg formula for He  $^1P^o$   $v^A = 0^+$  state energies has the form (in a.u., relative to the double-escape threshold):

$$E(N, n) = -\frac{2}{N^2} - \frac{1}{2(n - \mu_N)^2}, \quad (1)$$

where  $n = N, N+1, \dots$ , etc. The quantum number  $n$  is better regarded as a hyper-radial quantum number, rather than as an "outer electron principal quantum number" as in Herrick's work.<sup>14</sup> In Eq. (1) the  $n$ -independent quantum defect  $\mu_N$

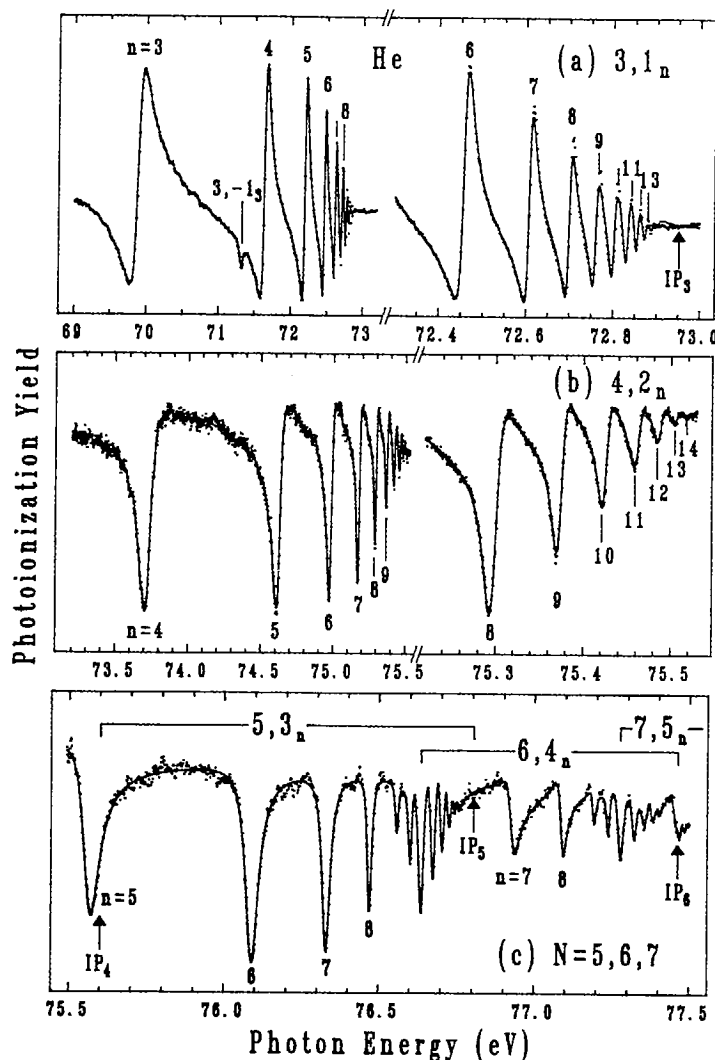


Fig. 3. Photoionization spectra of the helium atom as measured by Domke *et al.*<sup>1</sup> are shown as a relative cross section versus photon energy in eV. (a) below the  $N = 3$  threshold  $IP_3$ ; (b) below the  $N = 4$  threshold  $IP_4$ ; (c) below the  $N = 5$  and  $N = 6$  thresholds  $IP_5$ ,  $IP_6$ . The high- $n$  regions are shown magnified on the right-hand sides of (a) and (b). In (c) the different  $N$ -manifolds overlap and perturb each other.

(1)

regarded as a hyper-  
principal quantum  
quantum defect  $\mu_N$

is defined by

$$\mu_N = N - \frac{1}{\sqrt{\frac{2(2-\sigma)^2}{(N-\mu)^2} - \frac{4}{N^2}}}. \quad (2)$$

with  $\sigma$  the same screening parameter used by Rau<sup>9</sup> and Read.<sup>8</sup> Similarly  $\mu$  is the same constant (two-electron) quantum defect used in Refs. 8 and 9. These two parameters are adjusted to fit the sequence of Wannier ridge states only, namely those having comparable radial excitation of both electrons  $n = N$ . Fitted values of the parameters are  $\sigma = 0.1587$  and  $\mu = -0.1815$ .<sup>1</sup> Figure 4(a) shows how this formula accurately describes the lower observed resonances in helium, and Fig. 4(b) shows how its modified version for  $H^-$  is comparably successful.

For  $H^-$ , the outermost electron is not Rydberg-like, because it experiences no net Coulombic charge as it roams far from the hydrogen residue in state  $N$ . But because of the accidental degeneracy of different partial waves  $\ell$  in hydrogen, the outermost electron experiences a permanent dipole potential caused by the degenerate Stark-type mixing of those states. As is well known from the work of Gailitis and Damburg<sup>15</sup> and others, such a permanent dipole potential  $-a/2r^2$  can support an infinite series of levels when the dipole moment is sufficiently attractive  $a > \frac{1}{4}$ . For the  $0^+ \ ^1P^\circ$  levels of  $H^-$ , degenerate perturbation theory can be used to show that the relevant dipole moments for this propensity-favored channel attached to the  $N$ -th hydrogen threshold are given to about 1% accuracy by

$$a_N \approx 3N^2 - \frac{23N}{3} + 1 + \frac{2}{3N}. \quad (3)$$

The energies of an infinite number of dipole states are characterized most simply in terms of the related parameter  $\alpha_N \equiv \sqrt{a_N - \frac{1}{4}}$ . Following logic similar to

that used above for helium then leads to the following form of the two-electron Rydberg-dipole resonances expected for  $H^-$ :

$$E(N, n) = -\frac{1}{2N^2} - \exp\left(\frac{-2\pi(n-N)}{\alpha_N}\right) \left(\frac{(1-\sigma)^2}{(N-\mu)^2} - \frac{1}{2N^2}\right). \quad (4)$$

In Eqs. (1) and (4), the convention has been used that the integer quantum number  $n$  obeys  $n \geq N$ . Fitted values for the two empirical parameters are  $\sigma = 0.1629$  and  $\mu = -0.3423$  for  $H^-$ .<sup>3</sup>

Reference 3 pointed out that an immediate prediction of this two-electron resonance position formula is that for sufficiently high  $N$ , the lowest (Wannier ridge-) state in the  $N$ -manifold having  $n = N$  will fall below the  $N-1$  threshold. When this happens, this level will be quasi-degenerate with the entire series of high-lying one-electron Rydberg levels converging to the  $N-1$  ionization threshold, or in the case of  $H^-$  it will be quasi-degenerate with the series of high-lying dipole levels attached to the threshold  $N-1$ . In the adiabatic hyperspherical approximation, the  $n = N$  level would not interact with the high-lying levels attached to the  $N-1$  threshold, but in the actual He or  $H^-$  this interaction will be present and it will be important. The result of the interaction is that the  $n = N$  level will become distributed among all of the  $N-1, n'$  levels, causing their quantum defects to increase by unity as the width of the perturber is crossed.

(2)

and.<sup>8</sup> Similarly  $\mu$  is the  
8 and 9. These two  
states only, namely  
 $n = N$ . Fitted values  
4(a) shows how this  
in helium, and Fig.  
successful.

because it experiences  
a residue in state  $N$ .  
waves  $\ell$  in hydrogen,  
potential caused by the  
known from the work  
hole potential  $-a/2r^2$   
moment is sufficiently  
perturbation theory  
is propensity-favored  
to about 1% accuracy

(3)

characterized most simply  
logic similar to  
m of the two-electron

$$\left( \frac{1}{2} - \frac{1}{2N^2} \right). \quad (4)$$

the integer quantum  
parameters are

this two-electron res-  
vest (Wannier ridge-)  
 $-1$  threshold. When  
series of high-lying  
threshold, or in the  
high-lying dipole levels  
practical approximation,  
attached to the  $N-1$   
the present and it will  
 $N$  level will become  
quantum defects to

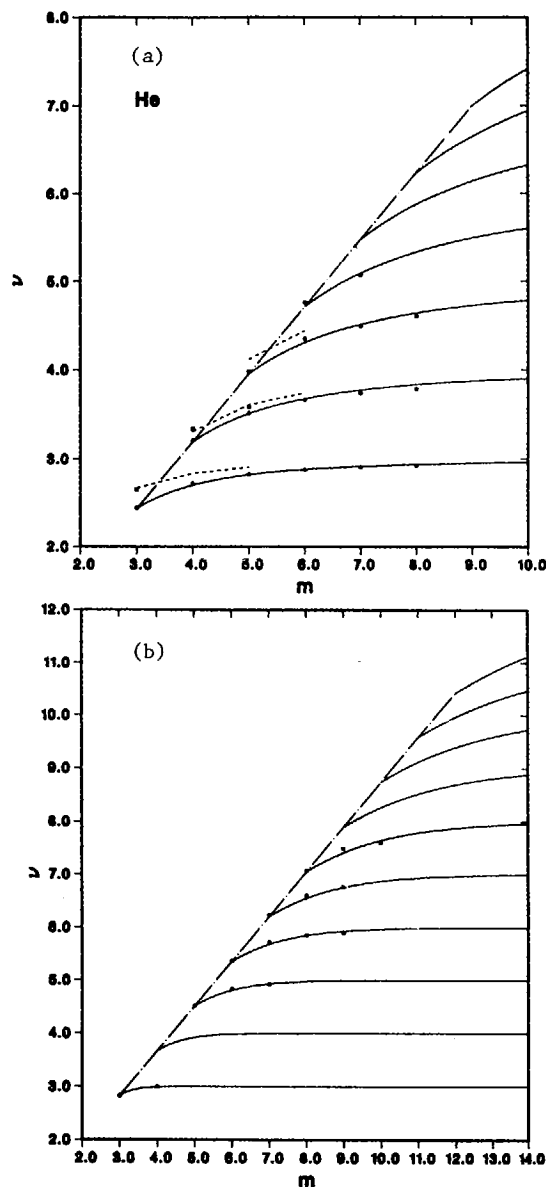


Fig. 4. Comparison of observed energies of  $1P^\circ$  resonances in (a) He, and (b)  $H^-$ , on an effective quantum number scale, with the prediction of two-electron Rydberg formulas given in the text. These are shown as solid curves for the propensity-favored  $v = 0$  states, and as a short-dashed curve for  $v = 1$  states of He in (a) only. The abscissa  $m$  of (a) and (b) is the number of nodes of the wavefunction in the hyper-radius  $R$  added to the hydrogenic manifold quantum number  $N$ , which was denoted  $n$  in Eqs. 1 and 4 and in the rest of this paper. From Refs. 3 and 4.

The basic physics of a perturber embedded in a Rydberg series, which is in turn embedded in an autoionization continuum, is efficiently described by three-channel quantum defect theory. The short-range parameters of MQDT were fitted in Ref. 2 to the experimental cross section, and are shown as a solid line along with the data in Fig. 3(a). The agreement suggests that this interpretation is correct: namely that the experiment is observing a perturbation of the  $N = 5$   $0^+$  Rydberg series by the  $N = 6$  Wannier ridge state of  $0^+$  character. Apparently, despite the greater complexity of the spectrum in the presence of such perturbations, the basic propensity rule for exciting predominantly the  $v^A = 0^+$  channel remains valid. It will be highly desirable to develop theoretical methods to the point where they can calculate the spectrum of Fig. 3 *ab initio*, in order to test this interpretation more stringently. Detailed studies of these double excitations in He and  $H^-$  are discussed in the next section, from the perspective of quantum defect theory and the eigenchannel R-matrix method.

### QUANTITATIVE CALCULATIONS OF THE PHOTOABSORPTION SPECTRUM

The great majority of studies of two-electron systems in recent years have been of the *qualitative* or *semiquantitative* variety. The aim has been to find a theoretical formulation that explains the striking simplicity of the observed propensity rules. Some success has been achieved using hyperspherical methods, molecular models, group theoretical schemes, and even classical (Newtonian) analyses. While much has been accomplished using these methods, all of them are ultimately disappointing at some level. For instance, the adiabatic hyperspherical interpretations neglect certain nonadiabatic coupling terms, without giving a detailed justification. Indeed, one of the puzzles of the hyperspherical interpretation all along has been the fact that calculations of these nonadiabatic coupling terms show them to be nonnegligible. A similar puzzle arises in the molecular model of Feagin, Briggs, and Rost,<sup>6</sup> who treat the motion of the electron pair as being "adiabatic" relative to the motion of the nucleus in a two-electron atom. This viewpoint, while seemingly counterintuitive, provides a good description of the qualitative nodal structure of these resonances. However, it has poorer quantitative accuracy than the adiabatic hyperspherical treatment when it comes to actually calculating energy levels. In similar fashion, the group theoretical work of Herrick and coworkers<sup>12</sup> assumes that the two-electron wave functions can be sorted out as eigenfunctions of the Casimir operators of the group  $SO(4) \times SO(4)$ . While some sensible interpretations result from this assumption, including the  $K, T$  quantum numbers, its physical basis, its range of validity, and its quantitative justification still remain unknown.

To address these limitations of the adiabatic and group theoretical schemes, we have initiated a quantitative description of these two-electron atoms, making use of multichannel quantum defect theory (MQDT)<sup>16</sup> and the eigenchannel R-matrix approach.<sup>7,17</sup> In recent years this approach has been highly successful in calculating and interpreting spectra of the doubly-excited alkaline earth atoms. A detailed description of this variational description of a correlated atomic system can be found in Refs. 7 and 17. Here we only summarize the main ideas.

The portion of configuration space over which two electrons can interact is



series, which is in  
described by three-  
MQDT were fitted  
solid line along with  
station is correct:  
= 5 0<sup>+</sup> Rydberg  
ently, despite the  
ations, the basic  
remains valid. It  
point where they  
his interpretation  
n He and H<sup>-</sup> are  
defect theory and

HE

t years have been  
o find a theoret-  
erved propensity  
methods, molecu-  
onian) analyses.  
m are ultimately  
pherical interpre-  
giving a detailed  
interpretation all  
pling terms show  
model of Feagin,  
eing "adiabatic"  
This viewpoint,  
f the qualitative  
titative accuracy  
ctually calculat-  
k of Herrick and  
oe sorted out as  
(4). While some  
e *K, T* quantum  
itive justification

oretical schemes,  
n atoms, making  
eigenchannel R-  
hly successful in  
earth atoms. A  
d atomic system  
in ideas.  
s can interact is

limited in its radial extent. We use independent-electron coordinates to describe the distance  $r_i$  of the  $i$ -th electron from the nucleus and its orientation  $\theta_i, \phi_i$  relative to some fixed axis in space. For a two-electron system at energies below the double-escape (or Wannier) threshold, the two electrons can exchange energy, spin, and angular momentum only over a finite region. The shape of this region is somewhat ambiguous and in any case not very important. The main point is that a reaction volume radius  $r_0$  can be identified at any energy such that when either electron moves beyond  $r_0$  it no longer exchanges energy with the residual electron. The order of magnitude of  $r_0$  is  $5N^2/Z$ , for treating two electrons in the field of an ion of charge  $Z$ , up to energies near  $-Z^2/2N^2$  a.u. Within this finite volume of configuration space the eigenchannel R-matrix method amounts to diagonalizing the Hamiltonian (plus the Bloch reaction surface operator) in a fairly large basis (typically a few hundred basis functions). The eigenvalues and eigenvectors are used to construct a variational approximation to the logarithmic derivative matrix (or R-matrix) on the surface of this reaction volume. In such calculations, at most one electron is assumed to escape from the reaction volume at any given time, an approximation that cannot treat double-escape processes. This is the major limitation of this approach at present.

It is crucial to account for the accidental degeneracy of the hydrogenic one-electron level left behind by an escaping electron. In physical terms, this degeneracy of different orbital momenta  $\ell$  permits the two electrons to exchange angular momenta even when the outermost electron roams to very large distances. This is efficiently done using the dipole representation of Gailitis and Damburg,<sup>15</sup> in conjunction with generalized quantum defect theory.<sup>18</sup> The basic idea of quantum defect theory in this context is to use the fact that solutions in the long-range dipole potential experienced by the outermost electron in H<sup>-</sup> are known to belong to the Bessel class (with real or imaginary order, depending on whether the effective dipole moment in a given channel is repulsive or attractive). For He, the electron moves in a combined Coulombic and dipolar potential, and the solutions are somewhat more complicated but still are the comparatively simple confluent hypergeometric functions. In any case, the basic concepts developed in Seaton's MQDT<sup>16</sup> carry over to any long-range potential, although the detailed formulae are somewhat different depending on the particular long-range potential in any given channel.<sup>18</sup>

Evidence that this procedure is capable of describing the H<sup>-</sup> resonance physics to spectroscopic accuracy is shown in the comparison of theory and experiment in Fig. 5, in several different energy ranges. The *ab initio* theoretical spectra are from the combined eigenchannel R-matrix and MQDT calculation of Sadeghpour *et al.*<sup>19</sup> The experimental spectra in Fig. 5 were obtained from the LAMPF experiments of Hamm *et al.*<sup>20</sup> and of Halka *et al.*<sup>21</sup> Our primary interest is in testing various propensity rules than in reproducing such spectra, but the agreement between theory and experiment in Fig. 5 gives us some confidence that our conclusions about the propensity rules can be trusted. This can be done using some of the intermediate quantities that occur in the calculation of the photoionization cross section, such as the  $^1P^o$  portion of the physical scattering matrix  $S_{ii'}(E)$  at the final state energy  $E$ . The qualitative picture of the photoexcitation of these high-lying doubly-excited states that emerged from Refs. 1-4 and other studies is that the photoabsorption initially excites the lowest few channels only at com-

paratively small distances. As a result, only channels with  $v = 0$  are appreciably excited at small distances. Immediately thereafter, the two electrons move outward as a consequence of their large kinetic energy. In the hyperspherical picture they make a sequence of nonadiabatic transitions to successively higher potential curves. If no such transitions are made, only the hydrogenic  $1s$ -state is excited and the high-lying doubly-excited resonances will not be reached at all. It is these nonadiabatic transitions which appear to have a strong propensity to conserve the quantum numbers  $v$ ,  $A$ , and  $T$ . A prediction suggested by this qualitative picture is that the "time reversed process" of autoionization of a doubly-excited state will similarly conserve those same quantum numbers approximately. Moreover, because the nonadiabatic (Landau-Zener-type) transitions tend to occur mostly between adjacent potential curves, the autoionization decay occurs primarily into the closest continuum in energy having the propensity-favored quantum numbers. For example, the lowest  $H^-$   $N = n = 4$  Wannier ridge state of  $v^A = 0^+$  character should mostly decay into the  $N = 3$  continuum of  $0^+$  character.

One way to test such propensity rules is to examine the partial photoionization cross sections into all the available escape channels. This can be somewhat difficult to interpret, as stressed in Ref. 19, because the partial cross sections can be reached via a complicated mixture of direct-photoionization pathways and pathways through the autoionizing levels. Moreover, the partial cross sections can depend strongly on the initial state being photoionized, whereas the propensity rules are more a statement about channel interactions in the final state alone, which should be *independent* of the initial state. In fact, Smith<sup>22</sup> developed a

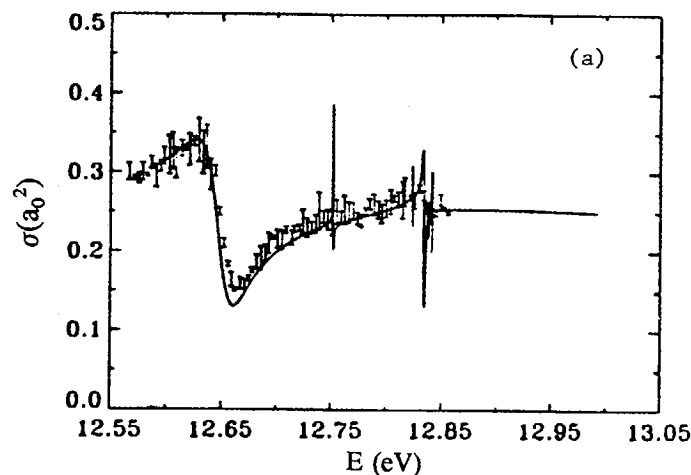
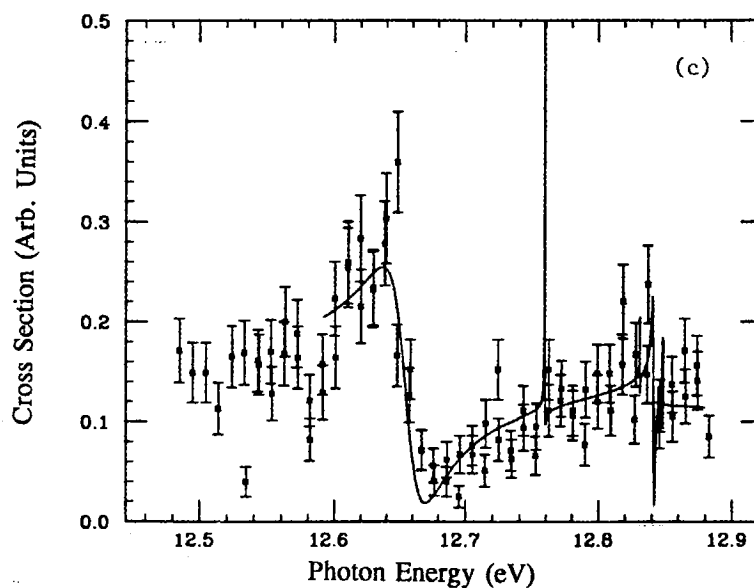
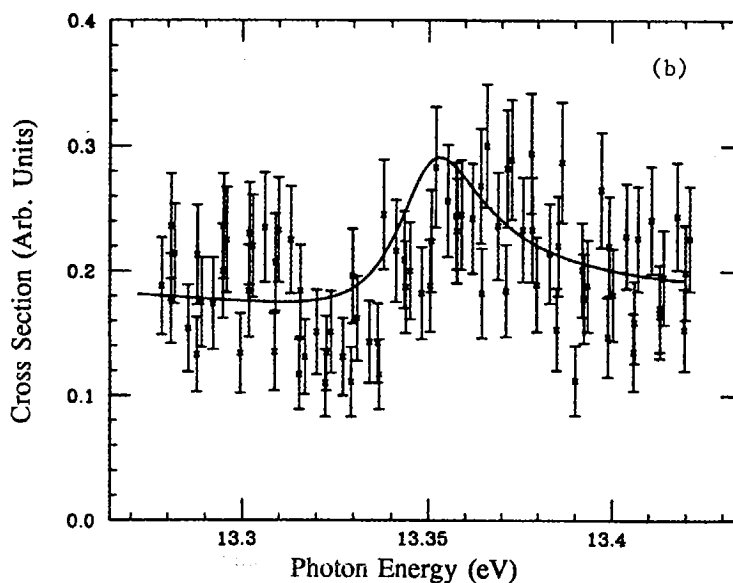


Fig. 5. Comparison of relative  $H^-$  photodetachment cross sections measured at LAMPF with the theoretical spectra obtained from the eigenchannel R-matrix and quantum defect calculation of Ref. 19. (a) Total photodetachment cross section below the  $N = 3$  threshold; (b) Partial photodetachment cross section for production of hydrogenic  $N = 2$  states, in the same energy range below  $H(N = 3)$  as in (a); (c) Partial cross section for production of  $H(N = 2)$ , except at higher energies below the  $N = 4$  detachment threshold. From Refs. 19-21.

$= 0$  are appreciably  
electrons move out-  
perspherical picture  
ely higher potential  
c 1s-state is excited  
ed at all. It is these  
nsity to conserve the  
s qualitative picture  
doubly-excited state  
timately. Moreover,  
end to occur mostly  
ccurs primarily into  
l quantum numbers.  
f  $v^A = 0^+$  character  
er.

partial photoioniza-  
is can be somewhat  
artial cross sections  
ation pathways and  
al cross sections can  
reas the propensity  
ne final state alone,  
mith<sup>22</sup> developed a



sections measured at  
enchannel R-matrix  
stodetachment cross  
ent cross section for  
nge below  $H(N=3)$   
(2), except at higher  
19-21.

useful analysis of just this problem when he introduced the *delay-time* matrix,

$$Q \equiv -i\hbar S^\dagger \frac{dS}{dE}. \quad (5)$$

Near an isolated resonance energy  $E_0$ , the delay time matrix  $Q$  can be shown to be a separable matrix, with a single dominant eigenvalue  $q_{max}$  displaying a Lorentzian peak of the form

$$q_{max}(E) = \frac{\Gamma}{(E - E_0)^2 + (\Gamma/2)^2}, \quad (6)$$

where  $\Gamma$  is the full width at half maximum. The squared components of the dominant eigenvector give the relative probabilities  $p_i$  for decay of the resonance state into the various allowed continuum channels  $i$ . The so-called "partial decay widths" into the various channels  $i$  are then given by  $p_i\Gamma$ . (This should not be interpreted as implying that the resonance width appears to be different when viewed in different observable channels, as in fact the width in energy of the resonance for every partial cross section is equal to the total  $\Gamma$ .)

Some examples of the results of this delay-time analysis for specific resonances of  $H^-$  follow. We use the following notation for these  $^1P^o$  channels involved, labeling each by  $Nv^A$ . Individual resonances will be classified by a channel label and by a "hyper-radial quantum number  $n$ " i.e. as  $Nv_n^A$ . More precisely, the quantum number  $n$  indicates that the number of nodes in the hyperspherical radius  $R$  is  $n - N + T - 1$  (for these  $^1P^o$  channels). The famous shape resonance  $20_2^+$ , lying just above the  $N = 2$  threshold, is found to decay 89% of the time into its own continuum  $20^+$ , as expected for a shape resonance whose decay width is primarily a result of intrachannel tunneling. This agrees with the hyperspherical interpretation given by Lin.<sup>23</sup> The remaining resonances analyzed are all Feshbach resonances, such as the lowest resonance shown in Fig. 5(a), namely the  $30_3^+$  resonance. This state is found to decay 89% of the time into the next lowest + continuum channel,  $20^+$ , and less than 5% into the three remaining accessible continua. The first Wannier ridge state below the  $N = 4$  threshold is  $40_4^+$ , and it decays 73% of the time into the adjacent propensity-favored continuum  $30^+$ , but a non-negligible 18% of the time it decays into the  $20^+$  continuum. Finally, the - state  $40_5^-$  which is very hard to excite from the ground state is found to decay 96% of the time into the expected channel  $30^-$ .

From such studies of these and other resonances in  $H^-$  and He, we have been able to piece together a semi-quantitative *hierarchy* of the validity of different propensity rules for nonadiabatic transitions. This tentative hierarchy reads as follows:

- (i) The strongest propensity rule is for the  $A$  quantum number. Scattering processes which change  $A$ , e.g. from + to -, occur only with probability in the range 0.005-0.05. For  $^1P^o$  symmetry, a change in  $A$  is equivalent to a change in  $T$ , so we have no separate information about  $\Delta T \neq 0$  propensity-unfavored processes.
- (ii) The next-strongest propensity rule is for the  $v$  quantum number. We have comparatively few examples of  $\Delta v \neq 0$  transitions, but their probability appears to be in the range 0.05 - 0.1 compared to propensity-favored transitions.
- (iii) Finally, the weakest of the propensity rules seen so far is the one indicating that processes having  $\Delta N = \pm 1$  tend to dominate. Violations of this propensity

delay-time matrix,

(5)

matrix  $Q$  can be shown  
value  $q_{max}$  displaying a

(6)

ed components of the  
decay of the resonance  
o-called "partial decay  
(This should not be  
to be different when  
width in energy of the  
al  $\Gamma$ .)

for specific resonances  
 $P^o$  channels involved,  
ied by a channel label  
. More precisely, the  
in the hyperspherical  
amous shape resonance  
y 89% of the time into  
whose decay width is  
with the hyperspherical  
alyzed are all Feshbach  
5(a), namely the  $30_3^+$   
e into the next lowest  
e remaining accessible  
threshold is  $40_4^+$ , and it  
ed continuum  $30^+$ , but  
ntinuum. Finally, the  
state is found to decay

and He, we have been  
e validity of different  
ive hierarchy reads as

mber. Scattering pro-  
probability in the range  
t to a change in  $T$ , so  
-unfavored processes.  
um number. We have  
eir probability appears  
ed transitions.  
r is the one indicating  
ions of this propensity

rule seem to occur with probability in the vicinity of 0.25. It should be pointed out that higher energy autoionizing resonances, such as the  $60_6^+$  Wannier ridge state of helium which falls below the  $N = 5$  ionization threshold,  $\Delta N = -1$  transitions are forbidden energetically to lead to autoionization. This propensity rule then reflects the dominant interactions among *closed channels*, rather than relative autoionization probability.

The large (25%) departure from the  $\Delta N = \pm 1$  propensity rule is somewhat surprising. A possible explanation, accounting for up to half of these processes resulting in  $\Delta N = -2$ , is that in decay to the propensity-favored  $\Delta N = -1$  continuum, the system has a 50% chance to be moving *inward* in  $R$  after the transition. If so, it may undergo a *second* propensity-favored nonadiabatic transition into the  $\Delta N = -2$  continuum. Since inelastic scattering at a single propensity-favored avoided crossing typically occurs with probability of about 20–30%, one expects such a two-step sequential process to cause  $\Delta N = -2$  autoionizing transitions with probability 10–15%. This does not explain the full 25% decay probability of the  $N = 4$  Wannier ridge resonance into the  $N = 2$  continuum, but perhaps accounts for half of this surprisingly large propensity-unfavored decay probability.

In summary, quantitative studies of the channel-interaction propensities along the lines discussed above promise to give a deeper understanding of the approximate selection rules operating in two-electron systems. Important directions to pursue include the extension of these methods to account for the more complicated perturbed Rydberg spectra characteristic of He and  $H^-$  at higher energies, as shown in Fig. 3. Explorations for the alkaline earth atoms and the isoelectronic alkali negative ions will be useful to further delineate the general validity (or lack thereof) of these approximate propensity rules.

## ACKNOWLEDGMENT

The work discussed here was supported by the Division of Chemical Sciences, Office of Basic Energy Sciences, U. S. Department of Energy.

## REFERENCES

1. M. Domke, C. Xue, A. Puschmann, T. Mandel, E. Hudson, D. A. Shirley, G. Kaendl, C. H. Greene, H. R. Sadeghpour, and H. Petersen, *Phys. Rev. Lett.* **66**, 1306 (1991).
2. P. G. Harris, H. C. Bryant, A. H. Mohagheghi, R. A. Reeder, H. Sharifian, C. Y. Tang, H. Tootoonchi, J. B. Donahue, C. R. Quick, D. C. Rislove, W. W. Smith, and J. E. Stewart, *Phys. Rev. Lett.* **65**, 309 (1990); P. G. Harris *et al.*, *Phys. Rev. A* **42**, 6443 (1990).
3. H. R. Sadeghpour and C. H. Greene, *Phys. Rev. Lett.* **65**, 313 (1990).
4. H. R. Sadeghpour, *Phys. Rev. A* **43**, 5821 (1991).
5. J. H. Macek, *J. Phys. B* **1**, 831 (1968); U. Fano, *Rep. Prog. Phys.* **46**, 97 (1983).

6. J. M. Feagin and J. S. Briggs, *Phys. Rev. Lett.* **57**, 984 (1986); also *Phys. Rev. A* **37**, 4599 (1988); J. M. Rost and J. S. Briggs, *J. Phys. B* **22**, 3587 (1989); J. M. Rost, J. S. Briggs, and J. M. Feagin, *Phys. Rev. Lett.* **66**, 1642(C) (1991).
7. C. H. Greene and M. Aymar, *Phys. Rev. A* **44**, 1773 (1991), and references therein.
8. F. H. Read, *J. Phys. B* **10**, 449 (1977).
9. A. R. P. Rau, *J. Phys. B* **16**, L699 (1983).
10. C. D. Lin and S. Watanabe, *Phys. Rev. A* **35**, 4499 (1987).
11. D. Wintgen, K. Richter, and G. Tanner, *Chaos* **2**, 19 (1992).
12. D. R. Herrick, *Adv. Chem. Phys.* **52**, 1 (1983).
13. C. D. Lin, *Adv. At. Mol. Phys.* **22**, 77 (1986).
14. D. R. Herrick and O. Sinanoglu, *Phys. Rev. A* **11**, 97 (1975).
15. M. Gailitis and R. Damburg, *Proc. Phys. Soc. Lond.* **82**, 192 (1963).
16. M. Seaton, *Proc. Phys. Soc. Lond.* **88**, 801 (1966); also *Rep. Prog. Phys.* **46**, 167 (1983).
17. C. H. Greene, *Phys. Rev. A* **28**, 2209 (1983); C. H. Greene and L. Kim, **38**, 5953 (1988), and references therein.
18. C. H. Greene, U. Fano, and G. Strinati, *Phys. Rev. A* **19**, 1485 (1979); C. H. Greene, A. R. P. Rau, and U. Fano, *Phys. Rev. A* **26**, 2441 (1982).
19. H. R. Sadeghpour, C. H. Greene, and M. Cavagnero, *Phys. Rev. A* **45**, 1587 (1992).
20. M. E. Hamm, R. W. Hamm, J. Bolton, D. A. Clark, H. C. Bryant, C. A. Frost, and W. W. Smith, *Phys. Rev. Lett.* **43**, 1715 (1979).
21. M. Halka, H. C. Bryant, E. P. Mackerrow, W. Miller, A. H. Mozhagheghi, C. Y. Tang, S. Cohen, J. B. Donahue, A. Hsu, C. R. Quick, J. Tiee, and K. Rozsa, *Phys. Rev. A* **44**, 6127 (1991).
22. F. Smith, *Phys. Rev.* **118**, 349 (1960).
23. C. D. Lin, *Phys. Rev. Lett.* **35**, 1150 (1975).